Alfarama Journal of Basic & Applied Sciences

Faculty of Science Port Said University

https://ajbas.journals.ekb.eg
ajbas@sci.psu.edu.eg
http://sci.psu.edu.eg/en/

January 2024, Volume 5, Issue I (Special Issue) DOI: 10.21608/AJBAS.2023.235429.1181

ISSN 2682-275X

Submitted: 16/09/2023
Accepted: 27/10/2023 Pages: 116 - 124

Structural Modification and Characterization of Sn-Zn Eutectic Alloy Doped with Copper Oxide Nanoparticles.

M.N. Gad[1,*], A.M. Abdelghany[2], Rizk Mostafa Shalaby[3], Tarek El Ashram[1]

[1]Faculty of Science, Port-Said University.

[2]Spectroscopy Department, Physics Research Institute, National Research Centre, 33 Elbehouth St., Dokki, 12311, Giza, Egypt

[3]Department of Physics, Faculty of Science, Mansoura University

***Corresponding author: mohamednazeih2@gmail.com**

ABSTRACT

It is well established that introducing nanoparticles into the solder metallic enhances its properties. This study aims to investigate the influence of adding a small amount of CuO nanoparticles on the microstructure, thermal properties, and electrical conductivity of environmentally friendly eutectic Sn90-x-Zn10-CuOx solder alloys. The solder alloys are prepared with varying CuO nanoparticle concentrations, specifically x = 0, 0.05, 0.1, 0.3, 0.5, and 1 wt. %. The study focuses on the evaluation of structure, thermal, and electrical properties, as well as the microstructure conditions of materials containing nanoparticles. To accomplish this, various techniques such as X-ray diffraction, and scanning electron microscopy were employed. X-ray diffraction and scanning electron microscopy were utilized to identify the phases present and examine the morphology features. Here we show that the microstructure investigations indicated that the incorporation of CuO nanoparticles into eutectic Sn-10Zn resulted in a reduction in crystallite size and led to finer and more homogeneous microstructure. Additionally, the addition of CuO nanoparticles led to an increase in the melting temperature and increased the electrical resistivity compared to the plain solder.

Keywords:

Lead-free solders; nanoparticles; microstructure; CuO NPs.

1. INTRODUCTION

Solder plays a crucial role in the assembly and interconnection of electronic materials, particularly in joining the silicon die or chip. It serves as a vital component that provides mechanical, thermal, and electrical continuity in electronic assemblies [1, 2]. The eutectic composition of lead-tin (Pb-Sn) solder has traditionally been widely used. but, due to the toxicity of lead, in 2006, the European Union RoHS directive mandated a strict prohibition on the utilization of lead (Pb) in the majority of electronic components due to the irreversible harm it poses to human health and environmental safety, particularly to Pb-based solder[3-5]. Sn-Zn solder alloys have been widely regarded as highly desirable alternatives to lead-based solders due to their low melting point, environmental friendliness, good electrical

conductivity, corrosion resistance, wide range of applications, and compatibility with different materials[6, 7]. There was a disagreement among researchers regarding the eutectic composition where it was confirmed the eutectic composition at 10 wt. % of Zn [8]. It will be established that the addition of nanoparticles enhanced the properties of solders [9-12].

Copper oxide is added to impart strength, corrosion resistance, heat resistance, wear resistance and machinability. Even small CuO additions of 0.5-1.0% can significantly enhance the properties and performance of alloys.

Therefore, this work aims to study the effect of the addition of CuO nanoparticles on the structure and properties of Sn-Zn eutectic solders.

2. EXPERIMENTAL PROCEDURES

2.1 Sample Preparation

The alloys were synthesized using high-purity Sn, Zn, and CuO nanoparticles (99.99% purity) supplied by DOP ORGANIK KIMYA SAN.VE TIC LTD.STI. To melt the alloys, a porcelain crucible was employed at 650°C. After 15 minutes of heating, the alloys were completely molten and manually agitated to enhance homogeneity. They were then returned to the furnace for an additional 30 minutes. The molten alloys were poured onto a rotating copper roller of the melt-spinning technique, which had a linear speed of 314 cm/s. The corresponding alloys produced lengthy ribbons that were 4 mm wide and about 55 μm thick.

2.2 Characterization Techniques

Various methods and techniques, such as X-ray diffraction (XRD), were used to examine the crystallography of melt-spun ribbons made from lead-free alloys. The microstructure was analyzed using a scanning electron microscope (SEM) [13]. The melting temperature had been determined using Differential scanning calorimetry (DSC). The electrical resistivity of **Sn90-x-Zn10-CuOx** NPs solder alloys was measured at different temperatures using the Bs407 Precision Milli/Micro Ohmeter.

3. RESULTS AND DISCUSSION

3.1 Structure Analysis

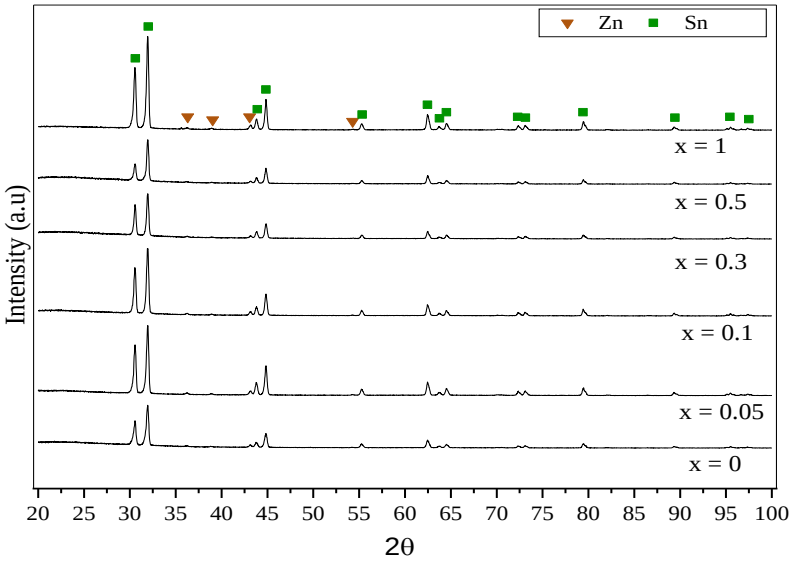

Fig.1 XRD patterns of **Sn90-x-Zn10-CuOx** NPs solders.

Fig.1 Shows the XRD patterns of **Sn90-x-Zn10-CuOx**NPs solder alloys. There are 13 Peaks of (β-Sn) and 4 peaks of (α-Zn). Phases are identified in the above-mentioned fingers corresponding to Tetragonal and Hexagonal systems respectively. CuO NPs had been dissolved in the Sn – Zn matrix so, the lattice

parameter had been changed significantly. X-ray peak broadening analysis was used to determine the crystalline size (D) and lattice strain (ε) using the Williamson-Hall relation[14]:

$$\beta \cos\theta = \frac{K\lambda}{D} + 4\varepsilon \sin\theta$$

Where β is the full width of half maximum, λ is the wavelength of x-rays and θ is the Bragg-angle. A plot has been drawn using 4 sin on the X-axis and cos on the Y-axis. The y-axis intercept of the linear fit to the data was used to calculate crystallite size, and the slope of the fit line was used to calculate lattice strain. Table 1 depicts the behavior of the axial ratio c/a, crystallite size, and lattice strain of **Sn90-x-Zn10-CuOx** NPs solder alloys. The results indicated that CuO NPs addition led to increasing the axial ratio c/a from 0.5447 for plain Sn-10Zn solder alloy to 0.5452 for **Sn90-x-Zn10-CuOx**NPs solder alloys, coinciding with reduced crystallite size (D) of (β-Sn) from 42.66 nm for plain Sn – 10Zn solder alloy to 37.47 nm. This is owing to the expanding of a-axis value where the c-axis is stiffest [15, 16]. Furthermore, the lattice distortion (ε), decreased to 2.724 X 10^{-4} at 1.0 wt. %.

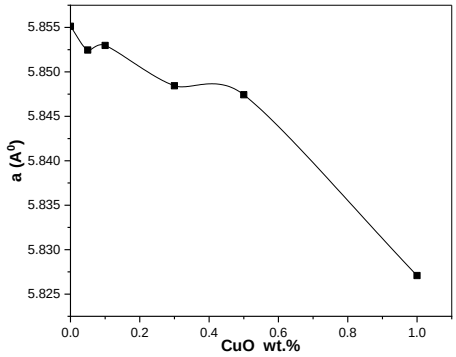

(a)

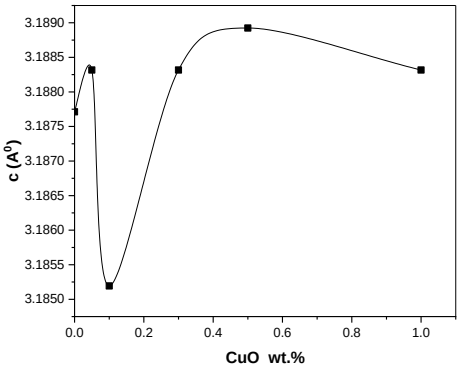

(b)

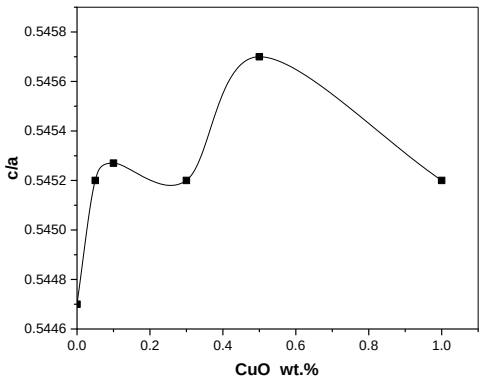

(c)

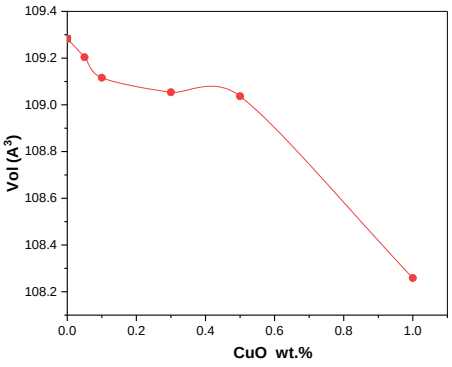

(d)

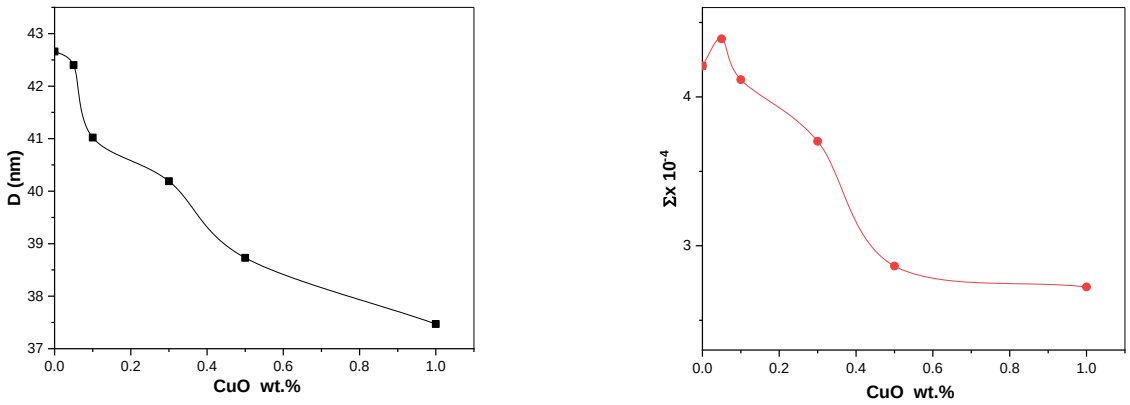

(e) (f)

Fig. 2 shows the effect of CuO NPs addition on (a) lattice parameter a, (b) lattice parameter c, (c) axial ratio, (d) volume of unit cell, (e) crystallite size, and (f) lattice strain of the eutectic solder alloys.

Table 1. Summarize lattice and cell parameters of **Sn90-x-Zn10-CuOx**NPs solder alloys.

Composition	a (Å)	c (Å)	c/a	V (Å^3)	D(nm)	ε x 10^{-4}
Sn-10Zn	5.85513	3.18771	0.5447	109.283	42.66	4.208
Sn-10Zn-0.05CuO	5.85246	3.18832	0.5452	109.204	42.4	4.390
Sn-10Zn-0.1CuO	5.85297	3.18519	0.5452	109.116	41.02	4.116
Sn-10Zn-0.3CuO	5.84844	3.18832	0.5452	109.054	40.19	3.702
Sn-10Zn-0.5CuO	5.84743	3.18892	0.5457	109.037	38.73	2.864
Sn-10Zn-1CuO	5.82708	3.18832	0.5452	108.259	37.47	2.724

3.2 Microstructure

Fig.3 (a-f) depicts the **Sn90-x-Zn10-CuOx**NPs solder alloys' solidified microstructures taken with SEM. The microstructure of **Sn90-x-Zn10-CuOx** alloys resembles the dendritic crystal structure of Sn (dominant phase) with irregularly shaped Zn particles submerged in it. One can see that, the grain size got finer and more flattened with the addition of a trace amount of CuO NPs compared to Sn-10Zn NPs-free; this may be owing to an alloy's adsorption phenomenon throughout the process of solidification. [15].
SEM shows a composite microstructure with nanoscale CuO particles distributed through the tin-zinc matrix to provide strengthening and other benefits to the alloy.

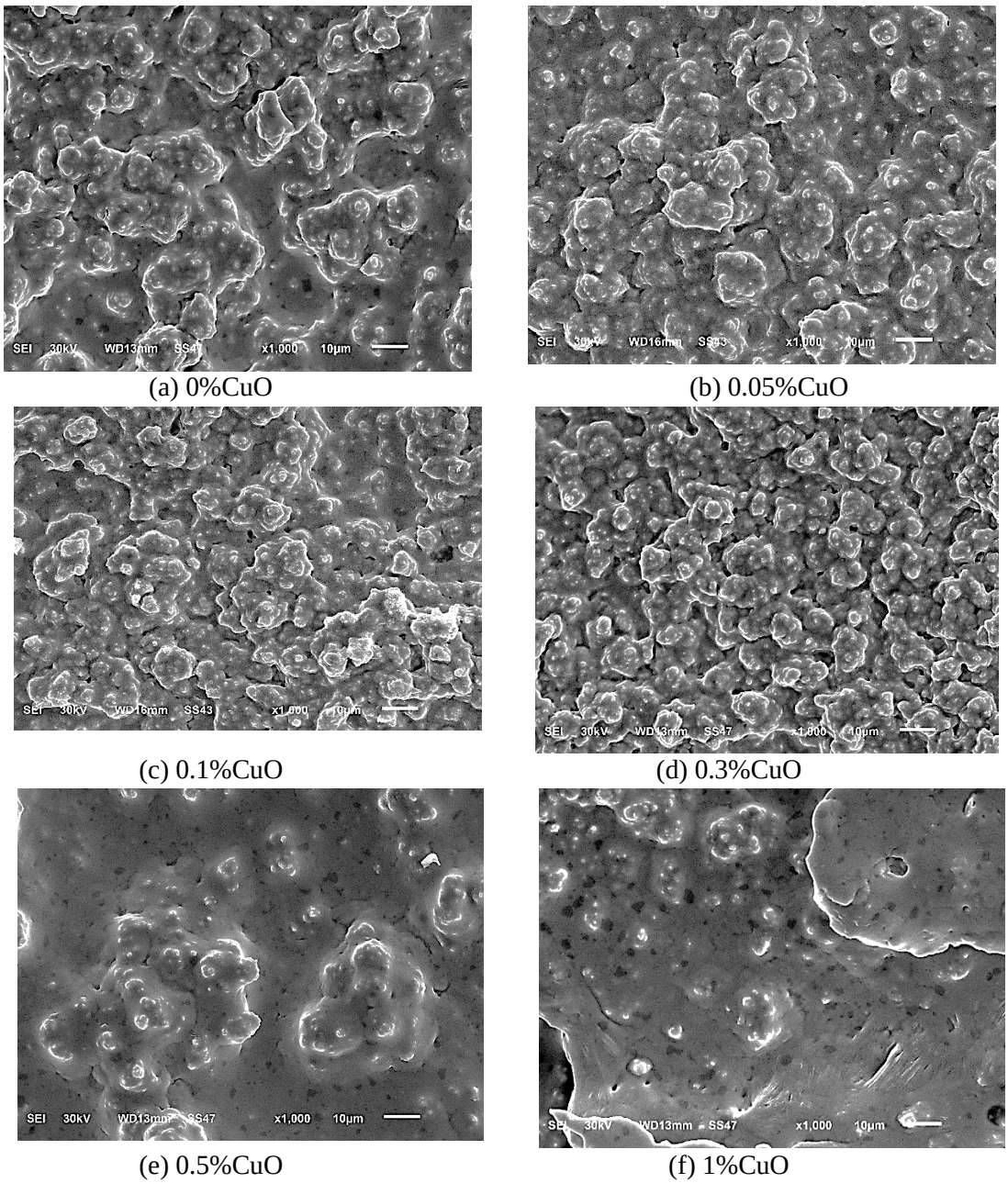

Fig.3 SEM microstructure of melt-spun**Sn90-x-Zn10-CuOx**(x= 0, 0.05, 0.1, 0.3, 0.5 and 1 wt. %) solder alloys

3.3 Thermal Properties

Figure 4 illustrates DSC curves resulting from Sn90-x-Zn10-CuOx NPs solder alloys when heated at a rate of 10^0K/min. Individual endothermic peak had been obtained related to the melting process. Solidus temperature (T_s), melting temp. (T_m), pasty range ($\triangle T$), liquidus temperature (T_l), and the enthalpy of fusion ($\triangle H_f$) were determined using these curves and are shown in Table 2. Melting is typically characterized as a non-continuous change from one phase to another and occurs when the free energy temp. of those phases are equal [17]. Compared to the eutectic Sn-10Zn solder alloy, the melting point of Sn90-x-Zn10-CuOx solder alloy increased with CuO NPs addition, which indicates the influence of CuO NPs on the structural properties of the alloy. Previous research has demonstrated that melting takes place when the RMS vibration amplitude of molecules exceeds a particular value that depends on the inter-

atomic distances [18]. Therefore, the observed increase in melting temperature of the nano-doped alloy compared to the Sn-10Zn solder alloy can attributed to a decrease in crystallite size and interatomic distance [19], [20].

CuO nanoparticle additions modify thermal conductivity, CTE, melting point, specific heat, thermal fatigue resistance and oxidation resistance. The tradeoffs have to be balanced based on the application requirements.

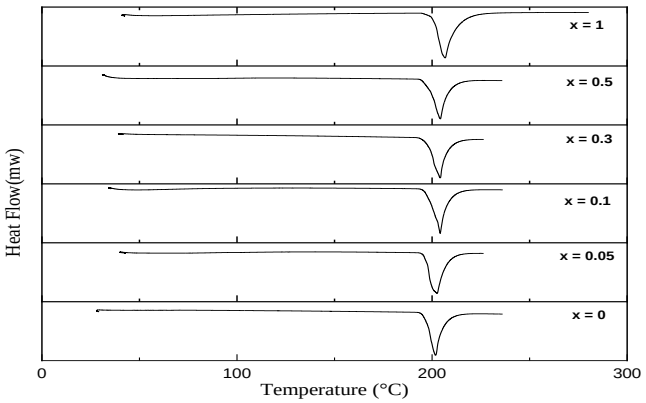

Fig.4.DSC curves for Sn_{90-x}-Zn_{10}-CuO_x NPs solder alloys where x=0, 0.05, 0.1, 0.3, 0.5 and 1 wt. %

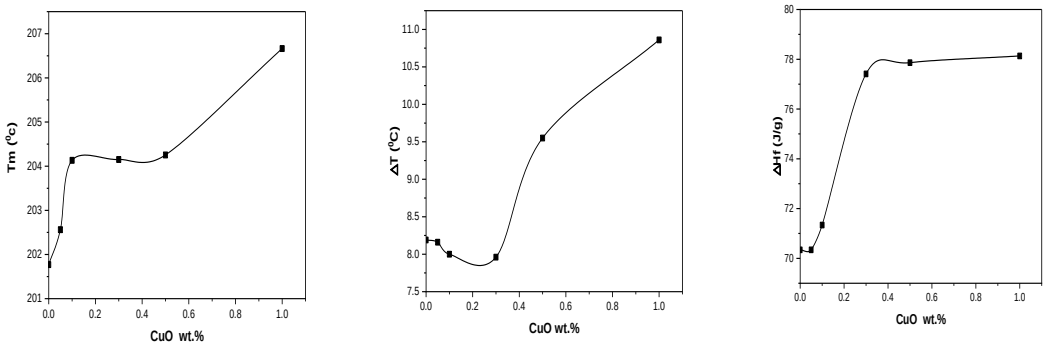

(a) (b) (c)

Figs. 5 (a, b, and c) show the effect of CuO NPs addition on (a) the melting temperature, (b) the pas range, and (c) the heat of fusion of the eutectic solder alloy

Table 2 Thermal characteristics of Sn_{90-x}-Zn_{10}-CuO_x solders during heating that heated at a rate of 10 °K/min

composition	T_m (°C)	T_s (°C)	T_l(°C)	△T (°C)	$\triangle H_f$(J/g)
Sn-10Zn	201.77	196.8	204.99	8.19	70.34
Sn-10Zn-0.05CuO	202.56	196.84	207	8.16	70.34
Sn-10Zn-0.1CuO	204.13	199.98	207.98	8.00	71.33
Sn-10Zn-0.3CuO	204.15	198.63	206.59	7.96	77.41
Sn-10Zn-0.5CuO	204.25	198.68	208.23	9.55	77.86
Sn-10Zn-1.0CuO	206.66	200.73	211.59	10.86	78.13

3.4 Electrical Properties

Fig. 6 shows the variation of electrical resistivityρ with temperature for Sn_{90-x}-Zn_{10}-CuO_x NPs solder alloys. During heating the resistivity increases linearly with temperature as for metallic behavior of metals and alloys. The resistivity at room temperature and the temperature coefficient of resistivity (TCR) were determined. Fig. 7a shows the variation of ρ with CuO concentration at room Temp. It is apparent that the electrical resistivity increases linearly by increasing the CuO concentration. This increase in electrical resistivity may be attributed to the presence of CuO molecules which can disrupt the crystal structure of the matrix, leading to scattering of electrons and hence increasing the resistivity[21]. Fig. 7b shows the variation of TCR with CuO concentration. TCR increases by increasing CuO concentration until it reaches a constant value at a higher concentration of CuO. This behavior may be due to that the scattering of conduction electrons by CuO molecules is more pronounced than the scattering from phonons. The values of resistivity at room temperature and TCR for Sn_{90-x}-Zn_{10}-CuO_x NPs solder alloys are shown in Table 3.

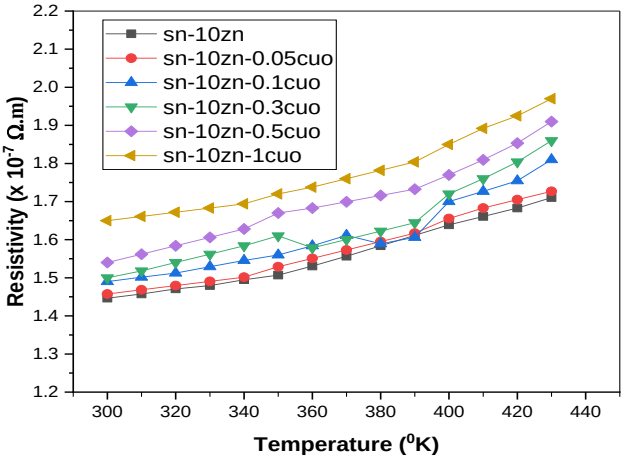

Fig. 6 The variation of electrical resistivity with the temperature for Sn_{90-x}-Zn_{10}-CuO_x NPs solder alloys.

(a) (b)

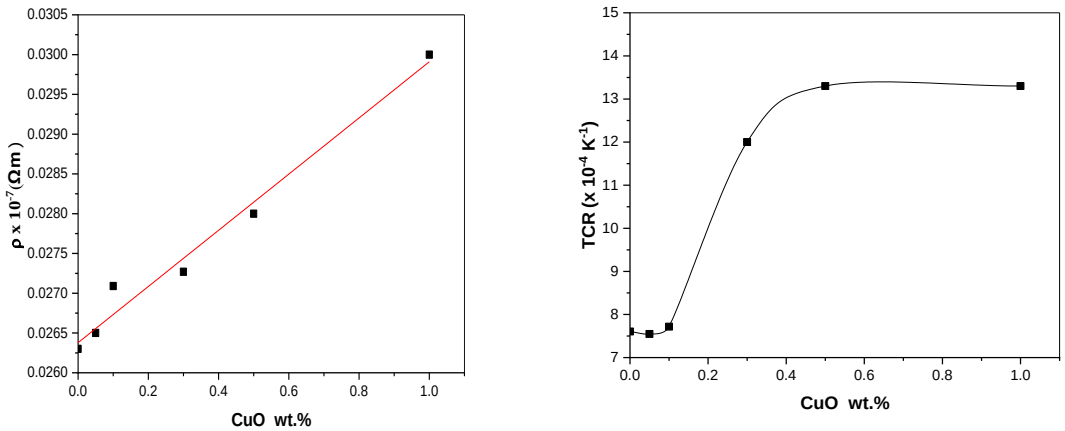

Fig. 7(a) the effect of CuO NPs addition on the electrical resistivity and (b) temperature coefficient of resistivity for eutectic solder alloys at 300°K.

Table 3 Electrical resistivity and conductivity of Sn_{90-x}-Zn_{10}-CuO_x NPs solder alloys

Alloys	ρ x10^{-7} (Ω.m)	TCR x 10^{-4} K^{-1}
Sn-10Zn	1.44	7.60
Sn-10Zn-0.05CuO	1.45	7.54
Sn-10Zn-0.1CuO	1.49	7.71
Sn-10Zn-0.3CuO	1.5	12.00
Sn-10Zn-0.5CuO	1.54	13.29
Sn-10Zn-1CuO	1.65	13.30

4. CONCLUSION

The study investigated the impact of CuO nanoparticles on the structure, microstructure, and thermal and electrical behavior of Sn_{90-x}-Zn_{10}-CuO_x solder alloys. The following important conclusions were drawn; Microstructural analysis demonstrated that the addition of CuO nanoparticles to the eutectic Sn - 10Zn causes the reduction and refinement of crystallite size. Results indicated that electrical resistivity and temperature coefficient of resistivity were increased with increasing CuO nanoparticle concentration as compared to the plain solder. Furthermore, the addition of CuO nanoparticles to the Sn-10Zn eutectic solder alloy resulted in a slight increase in the melting temperature and the enthalpy of fusion. In general, copper oxide is added to impart strength, corrosion resistance, heat resistance, wear resistance and machinability. Even small CuO additions of 0.5-1.0% can significantly enhance the properties and performance of alloys.

5. REFERENCES

[1] M. Abtew and G. Selvaduray, "Lead-free solders in microelectronics," *Materials Science and Engineering: R: Reports,* vol. 27, no. 5-6, pp. 95-141, 2000.

[2] S. Cheng, C.-M. Huang, and M. Pecht, "A review of lead-free solders for electronics applications," *Microelectronics Reliability,* vol. 75, pp. 77-95, 2017.

[3] J. Huang *et al.*, "Effect of deposition potential on electrodeposition of Sn-Ag-Cu ternary alloy solderable coating in deep eutectic solvent," *Journal of Electroanalytical Chemistry*, p. 117613, 2023.

[4] L. Zhang *et al.*, "Effects of trace amount addition of rare earth on properties and microstructure of Sn–Ag–Cu alloys," *Journal of Materials Science: Materials in Electronics,* vol. 20, pp. 1193-1199, 2009.

[5] B. Dompierre, V. Aubin, E. Charkaluk, W. C. Maia Filho, and M. Brizoux, "Influence of thermal ageing on cyclic mechanical properties of SnAgCu alloys for microelectronic assemblies," *Procedia Engineering,* vol. 2, no. 1, pp. 1477-1486, 2010.

[6] K. Subramanian, K. Suganuma, and K.-S. Kim, "Sn-Zn low temperature solder," *Lead-Free Electronic Solders: A Special Issue of the Journal of Materials Science: Materials in Electronics,* pp. 121-127, 2007.

[7] L. Zhang *et al.*, "Development of Sn–Zn lead-free solders bearing alloying elements," *Journal of Materials Science: Materials in Electronics,* vol. 21, pp. 1-15, 2010.

[8] M. Kamal, A. El-Bediwi, T. El-Ashram, and M. Dorgham, "VERIFICATION OF HUME-ROTHERY CONDITION OF PHASE STABILITY IN RAPIDLY SOLIDIFIED Sn-Zn BINARY ALLOYS," *Journal of Ovonic Research Vol,* vol. 7, no. 4, pp. 73-82, 2011.

[9] M.-l. Li, L. Zhang, N. Jiang, L. Zhang, and S.-j. Zhong, "Materials modification of the lead-free solders incorporated with micro/nano-sized particles: A review," *Materials & Design,* vol. 197, p. 109224, 2021.

[10] K. Kanlayasiri and N. Meesathien, "Effects of zinc oxide nanoparticles on properties of SAC0307 lead-free solder paste," *Advances in Materials Science and Engineering,* vol. 2018, 2018.
[11] P. Zhang, S. Xue, J. Wang, P. Xue, S. Zhong, and W. Long, "Effect of nanoparticles addition on the microstructure and properties of lead-free solders: a review," *Applied Sciences,* vol. 9, no. 10, p. 2044, 2019.
[12] P. Baumli, "Solder materials with micro and nanoparticles: a review," *MATERIALS SCIENCE AND ENGINEERING A Publication of the University of Miskolc,* vol. 40, no. 1, pp. 42-49, 2015.
[13] R. M. Shalaby, N. A. Abdelhakim, and M. Kamal, "Effect of rapid solidification on mechanical properties of free machining lead free aluminum alloys for improved machinability," *Journal of Advances in Physics,* vol. 13, no. 10, 2017.
[14] V. Mote, Y. Purushotham, and B. Dole, "Williamson-Hall analysis in estimation of lattice strain in nanometer-sized ZnO particles," *Journal of theoretical and applied physics,* vol. 6, pp. 1-8, 2012.
[15] R. M. Shalaby, M. Munther, A.-B. Al-Bidawi, and M. Kamal, "Effect of aluminum content on structure, transport and mechanical properties of Sn-Zn eutectic lead free solder alloy rapidly solidified from melt," *Journal: JOURNAL OF ADVANCES IN PHYSICS,* vol. 10, no. 1, 2015.
[16] D. Yu, J. Zhao, and L. Wang, "Improvement on the microstructure stability, mechanical and wetting properties of Sn–Ag–Cu lead-free solder with the addition of rare earth elements," *Journal of alloys and compounds,* vol. 376, no. 1-2, pp. 170-175, 2004.
[17] H. Al-sorory, M. S. Gumaan, and R. M. Shalaby, "Effect of TiO nanoparticles on the microstructure, mechanical and thermal properties of rapid quenching SAC355 lead-free solder alloy," *Soldering & Surface Mount Technology,* vol. 35, no. 1, pp. 18-27, 2023, doi: 10.1108/SSMT-01-2022-0003.
[18] F. Stacey and R. Irvine, "Theory of melting: thermodynamic basis of Lindemann's law," *Australian Journal of Physics,* vol. 30, no. 6, pp. 631-640, 1977.
[19] H. Al-sorory, M. S. Gumaan, and R. M. Shalaby, "Effect of TiO2 nanoparticles on the microstructure, mechanical and thermal properties of rapid quenching SAC355 lead-free solder alloy," *Soldering & Surface Mount Technology,* vol. 35, no. 1, pp. 18-27, 2023.
[20] J. Xian, Z. Ma, S. Belyakov, M. Ollivier, and C. Gourlay, "Nucleation of tin on the Cu6Sn5 layer in electronic interconnections," *Acta Materialia,* vol. 123, pp. 404-415, 2017.
[21] K. Karthik and N. V. Jaya, "High pressure electrical resistivity studies on Ni-doped TiO2 nanoparticles," *Journal of alloys and compounds,* vol. 509, no. 16, pp. 5173-5176, 2011.